AD-A047 184 NAVAL RESEARCH LAB WASHINGTON D C F/G 20/8
THE EFFECTS OF CROSS-SECTIONAL ELONGATION ON TRAPPED ELECTRON M--ETC(U)
SEP 77 K R CHU, E OTT, W M MANHEIMER E(49-20)1006
UNCLASSIFIED NRL-MR-3615 SBIE-AD-E000000 NL

| OF |

AD
A047184

END
DATE
FILMED
1 -78
DDC

(12)

AD-E000036

NRL Memorandum Report 3615

The Effects of Cross-Sectional Elongation on Trapped Electron Modes

K. R. Chu

Science Applications, Incorporated
McLean, Virginia 22101

Edward Ott

Department of Electrical Engineering
Cornell University, Ithaca, New York 14853

and

Wallace M. Manheimer

Plasma Dynamics Branch
Plasma Physics Division

September 1977

NAVAL RESEARCH LABORATORY
Washington, D.C.

(14) NRL-MR-3615

SECURITY CLASSIFICATION OF THIS PAGE (When Data Entered)

REPORT DOCUMENTATION PAGE

READ INSTRUCTIONS BEFORE COMPLETING FORM

1. REPORT NUMBER: ~~NRL Memorandum Report 3615~~

2. GOVT ACCESSION NO.

3. RECIPIENT'S CATALOG NUMBER (9)

4. TITLE (and Subtitle): (6) THE EFFECTS OF CROSS-SECTIONAL ELONGATION ON TRAPPED ELECTRON MODES

5. TYPE OF REPORT & PERIOD COVERED: Interim rep[redacted] ~~on a continuing NRL problem.~~

6. PERFORMING ORG. REPORT NUMBER

7. AUTHOR(s): (10) K. Chu, E. Ott, [redacted] W. Manheimer

R. ... ward ... Wallace M.

8. CONTRACT OR GRANT NUMBER(s): (15) E(49-20)-1006

9. PERFORMING ORGANIZATION NAME AND ADDRESS: Naval Research Laboratory, Washington, D.C. 20375

10. PROGRAM ELEMENT, PROJECT, TASK AREA & WORK UNIT NUMBERS: NRL Problem H02-37; Project ERDA E(49-20; 1006)

11. CONTROLLING OFFICE NAME AND ADDRESS: Energy Research and Development Admin., Washington, D.C. 20545

12. REPORT DATE: (11) Sep[redacted]77

13. NUMBER OF PAGES: (12) 22p.

14. MONITORING AGENCY NAME & ADDRESS (if different from Controlling Office): (18) SBIE (19) AD-E000 000

15. SECURITY CLASS. (of this report): UNCLASSIFIED

15a. DECLASSIFICATION/DOWNGRADING SCHEDULE

16. DISTRIBUTION STATEMENT (of this Report): Approved for public release; distribution unlimited.

17. DISTRIBUTION STATEMENT (of the abstract entered in Block 20, if different from Report)

18. SUPPLEMENTARY NOTES: This research was sponsored by Energy Research and Development Administration under Subtask (49-20:1006).

19. KEY WORDS (Continue on reverse side if necessary and identify by block number):

Tokamaks
Trapped electron modes
Cross-section
Elongation

20. ABSTRACT (Continue on reverse side if necessary and identify by block number):

The dispersion relation for the trapped electron mode in non-circular cross-section tokamaks is formulated and evaluated. It is shown that modest reductions in the growth rate result from cross-sectional elongation.

DD FORM 1 JAN 73 1473 EDITION OF 1 NOV 65 IS OBSOLETE
S/N 0102-014-6601

SECURITY CLASSIFICATION OF THIS PAGE (When Data Entered)

251950

CONTENTS

THE EFFECTS OF CROSS-SECTIONAL ELONGATION ON TRAPPED ELECTRON MODES

I. INTRODUCTION

Recently it has been shown[1] that the toroidal drift of trapped electrons can have a large destabilizing effect on the dissipative trapped electron mode. This is particularly true for high temperature regimes where the dissipation due to scattering of the trapped electrons becomes small. The destabilization may be viewed as resulting from a wave-particle resonance occuring when the toroidal component of the wave phase velocity is equal to the trapped particle toroidal drift. On the other hand, Glasser et al.[2] have shown that the cross-sectional elongation of a tokamak can slow down or reverse the toroidal trapped particle drift. Here we formulate and evaluate the relevant dispersion relation to study these effects.

Note: Manuscript submitted September 15, 1977.

II. COORDINATES

To begin, it is necessary to define the coordinate system. Let Ψ denote the poloidal magnetic flux function, such that surfaces of constant ψ are magnetic flux surfaces, and $d\psi = RB_\theta dl_\psi$, where B_θ is the poloidal component of $\underset{\sim}{B}$, R is the tokamak major radius coordinate, and dl_ψ is a differential length perpendicular to the flux surface. Also let θ be a coordinate denoting the poloidal position on a flux surface. We define θ by $d\theta = B_\zeta \left[q(\psi)RB_\theta(\theta)\right]^{-1} dl_\theta$, where B_ζ is the toroidal component of $\underset{\sim}{B}$, dl_θ is a differential length along the line of constant ψ in the poloidal plane, $q(\psi) = (2\Pi)^{-1} \int_c B_\zeta (B_\theta R)^{-1} dl_\theta$, and the subscript c on the integral symbol denotes integration over one circuit around the flux surface. Note that RB_ζ is constant on a flux surface. We assume that the mode is localized to a mode rational surface $q(\psi) \cong m/n$, where m and n are integers.

III. DISPERSION RELATION

We now turn to the formulation of the dispersion relation. We assume that the wave is purely electrostatic and neglect effects nonlocal in ψ (a treatment of shear stabilization in non-circular cross-section appears in Ref. 3). The perturbed distribution function F_j^1 for species j is given by the linearized Vlasov equation,

$$\frac{\partial}{\partial t}F_j^1 + \underset{\sim}{v}\cdot \frac{\partial}{\partial \underset{\sim}{x}}F_j^1 + \frac{q_j}{m_j c}\left(\underset{\sim}{v}\times\underset{\sim}{B}\right)\cdot \frac{\partial}{\partial \underset{\sim}{v}}F_j^1 = \frac{q_j}{m_j}\nabla\phi\cdot\frac{\partial}{\partial \underset{\sim}{v}}F_j^o , \tag{1}$$

where ϕ is the perturbed electrostatic potential, $\underset{\sim}{B}$ is the equilibrium magnetic field, and F_j^o, the equilibrium distribution function, is given by

$$F_j^o = F_j^M\left[1 - \frac{1}{\Psi_n}\left(1 - \frac{3}{2}\eta_j + \eta_j\frac{v^2}{v_j^2}\right)\left(\Psi - \frac{m_j Rc}{q_j}v_z\right)\right]. \tag{2}$$

In Eq. (2), F_j^M is the Maxwellian distribution function, $v_j \equiv (2T_j/m_j)^{\frac{1}{2}}$, $\Psi_n^{-1} \equiv - d\ell n\ n_o/d\Psi$, $\eta_j \equiv [d\ell n\ T_j/d\Psi]/[d\ell n\ n_o/d\Psi]$, and T_j, n_o are, respectively, the temperature and unperturbed electron or ion density.

Since we expect the wave electric field to be nearly perpendicular to $\underset{\sim}{B}$, we express the perturbation in the form

$$\phi = \hat{\phi}(\theta)\exp(im\theta - in\zeta - i\omega t) \tag{3}$$

where we expect $\hat{\phi}(\theta)$ to be a slow function of θ compared with the variation in the exponential part of Eq. (3). Since we employ the local approximation, any Ψ dependence of ϕ is neglected by Eq. (3).

a. Ion Response

To evaluate the ion density response, we substitute Eqs. (2) and (3) into Eq. (1) and integrate along unperturbed particle orbits,

$$F_i^1 = -\frac{e}{T_i}F_i^M \left\{ \phi + i\left[\omega + \frac{\omega_*}{\tau}\left(1 - \frac{3}{2}\eta_i + \eta_i\frac{v^2}{v_i^2}\right)\right] \cdot \int_{-\infty}^{t} dt' \hat{\phi}\left[\theta(t')\right] e^{im\theta(t') - in\zeta(t') - i\omega t'} \right\} \tag{4}$$

where $\omega_* \equiv nT_e c/e\Psi_n$, $\tau \equiv T_e/T_i$, and $e = |e|$ is the electron charge. In Eq. (4) we write the ion orbit as

$$\zeta(t') \cong \zeta + v_\parallel R^{-1}(t' - t), \tag{5}$$

$$\theta(t') \cong \theta + v_\parallel (Rq)^{-1}(t' - t) + \theta_\perp \tag{6}$$

$$\theta_\perp \cong v_\perp B_\zeta (qR\Omega_i)^{-1} \left\{ B_\theta^{-1}(t') \sin\left[\Omega_i(t'-t) + \beta\right] - B_\theta^{-1}(t)\sin\beta \right\}, \tag{7}$$

where β is the angle of $\underset{\sim}{v}$ with respect to the direction perpendicular to the flux surface, Ω_i is the ion cyclotron frequency, and we have assumed that $B_\zeta^2 >> B_\theta^2$ and a large aspect ratio so that Ω_i and B_ζ are approximately constant on a flux surface. Also we have assumed the scale length for changes in B_ζ perpendicular to a flux surface is long compared to an ion Larmor radius. Putting these orbits into Eq. (4) and making use of the identity $\exp(i\gamma \sin\alpha) = \sum_{n=-\infty}^{\infty} J_n(\gamma)\exp(in\alpha)$, where J_n is Bessel function of order n, we obtain for $\omega << \Omega_i$,

$$F_i^1 = -\frac{e\phi}{T_i} F_i^M - \frac{ie}{T_i}\left[\omega + \frac{\omega_*}{\tau}\left(1 - \frac{3}{2}\eta_i + \eta_i \frac{v^2}{v_i^2}\right)\right] F_i^M\, e^{im\theta - in\zeta}$$

$$\cdot \int_{-\infty}^{t} dt'\, \hat{\phi}\left[\theta(t')\right] J_o\left[\frac{nB_\zeta v_\perp}{R\Omega_i B_\theta[\theta(t')]}\right] J_o\left[\frac{nB_\zeta v_\perp}{R\Omega_i B_\theta(\theta)}\right] e^{-i\omega t'} . \qquad (8)$$

Note that the argument of the first Bessel function and $\hat{\phi}$ are to be evaluated following the orbit while the argument of the second Bessel function is evaluated at the Eulerian position. Since both $\hat{\phi}$ and J_o are not rapid functions of θ we may neglect $\theta_\perp$ in $\theta(t')$ appearing in Eq. (8). To evaluate the ion density we integrate Eq. (8) over all velocities. Interchanging the order of the t' and $v_\perp$ integrations yields

$$\frac{\delta n_i}{n_o} = -\frac{e\phi}{T_i} - i\frac{e}{T_i} e^{im\theta + in\zeta} \int_{-\infty}^{\infty} dv_\parallel \frac{\exp(-v_\parallel^2 / v_i^2)}{\pi^{\frac{1}{2}} v_i} \int_{-\infty}^{t} dt' e^{-i\omega t'}$$

$$\cdot \hat{\phi}(\theta') \left\{\left[\omega + \frac{\omega_*}{\tau}\left(1 - \frac{1}{2}\eta_i + \eta_i \frac{v_\parallel^2}{v_i^2}\right)\right] H(\alpha,\alpha') + \frac{\omega_* \eta_i}{2\tau} G(\alpha,\alpha')\right\} ,$$

where

$$H(\alpha,\alpha') \equiv \exp\left[-(\alpha^2 + \alpha'^2)/4\right] I_o(\alpha\alpha'/2) \quad ,$$

$$G(\alpha,\alpha') \equiv \exp\left[-(\alpha^2 + \alpha'^2)/4\right]\left[\alpha\alpha' I_1(\alpha\alpha'/2) - (\alpha^2 + \alpha'^2) I_o(\alpha\alpha'/2)/2\right] ,$$

$$\theta' \equiv \theta(t') \approx \theta + (t'-t)v_{\parallel}/Rq \quad ,$$

$$\alpha \equiv nB_{\zeta}v_i/R\Omega_i\, B_{\theta}(\theta) \qquad (9)$$

and

$$\alpha' \equiv nB_{\zeta}v_i/R\Omega_i\, B_{\theta}(\theta').$$

In obtaining the above, we have done the $v_{\perp}$ integration by making use of the integral

$$\int_0^{\infty} x dx \exp(-\rho^2 x^2) J_o(\alpha x) J_o(\beta x) = (2\rho^2)^{-1} \exp\left[-(\alpha^2 + \beta^2)/4\rho^2\right] I_o(\alpha\beta/2\rho^2).$$

In order to do the remaining integrations, we expand $\hat{\phi}$, G, and H in Fourier series

$$\hat{\phi}(\theta') = \sum_p a_p \exp(ip\theta') \qquad (10)$$

$$G(\alpha,\alpha') = \sum_{s,s'} g_{s,s'} \exp(is\theta + is'\theta')$$

$$H(\alpha,\alpha') = \sum_{s,s'} h_{s,s'} \exp(is\theta + is'\theta')$$

where

$$g_{ss'} = (2\pi)^{-2} \int_0^{2\pi} d\theta \int_0^{2\pi} d\theta'\, G(\alpha,\alpha') \exp(-is\theta - is'\theta')$$

and

$$h_{ss'} = (2\pi)^{-2} \int_0^{2\pi} d\theta \int_0^{2\pi} d\theta'\, H(\alpha,\alpha') \exp(-is\theta - is'\theta').$$

The t' integration is now easily done. Finally the $v_{\parallel}$ integration may be expressed in terms of the plasma dispersion function $Z(\xi)$,

$$Z(\xi) = \pi^{-\frac{1}{2}}\int_{-\infty}^{\infty} dx \exp(-x^2)/(x-\xi).$$

The result for $\delta n_i/n_o$ is

$$\frac{\delta n_i}{n_o} = \frac{-e}{T_i} \exp(im\theta-in\xi-i\omega t)\sum_{p,p'} a_{p'} M_{pp'} \exp(ip\theta) \tag{11}$$

where

$$M_{pp'} \equiv \delta_{pp'} + \frac{1}{\omega}\sum_s \left[\left(\omega + \frac{\omega_*}{\tau} - \frac{\eta_i\omega_*}{2\tau}\right)h_{s,p-p'-s} + \frac{\eta_i\omega_*}{2\tau} g_{s,p-p'-s}\right]\xi Z(\xi)$$

$$+ \frac{\eta_i\omega_*}{\tau} h_{s,p-p'-s} \quad \xi^2\left[1 + \xi Z(\xi)\right], \tag{12}$$

$\xi \equiv \omega Rq/(p-s)v_i$ and $\delta_{pp'}$ is the Kronecker delta. Equation (11) is our final result for the ion density perturbation. It can be shown that for circular cross section tokamaks (i.e., B_θ is independent of θ), M_{oo} reduces to previous results[1] while $M_{pp'}$ $(p \neq p')$ vanishes.

b. Electron Response

The electron density response is[4]

$$\frac{\delta n_e}{n_o} = \frac{e\phi}{T_e} - \frac{e}{T_e} \exp(im\theta-in\zeta-i\omega t)\int_T d^3\underset{\sim}{v} \frac{(\omega-\omega_{*e})F_e^M\langle\hat{\phi}(\theta)\rangle}{\omega-\omega_d(\lambda,v)+i\nu_{eff}(v)},$$

where $\omega_{*e} \equiv \omega_* (1-\frac{3}{2}\eta_e + \eta_e v^2/v_e^2)$, $\nu_{eff} \equiv \varepsilon^{-1}\nu_e(v_e/v)^3$

is the effective collision frequency for trapped electrons, ε is the inverse aspect ratio ($\varepsilon \equiv 1-B_{min}/B_{max}$), ν_e is the electron collision deflection frequency,[5] $\int_T$ denotes the velocity space integral over the trapped electrons, angle brackets denote bounce average, i.e. $\langle\hat{\phi}(\theta)\rangle = \tau_b^{-1}\oint dl_\theta(B/B_\theta)v_\parallel^{-1}\hat{\phi}(\theta)$, $\tau_b \equiv \oint dl_\theta(B/B_\theta)v_\parallel^{-1}$, $v_\parallel = v(1-\lambda B)^{\frac{1}{2}}$, $\lambda \equiv \mu(\frac{1}{2}m_e v^2)^{-1}$ specifies the velocity pitch angle of an electron, μ is the magnetic moment, $\oint$ denotes integration over the electron bounce orbit whose limits are defined by $\lambda B = 1$, $J \equiv \oint v_\parallel (B/B_\theta)\, dl_\theta$ is the longitudinal adiabatic invariant, and

$$\omega_d(\lambda,\nu) \equiv nm_e c(e\tau_b)^{-1}\partial J/\partial\psi. \tag{13}$$

Again using the expansion in Eq.(10), we obtain

$$\frac{\delta n_e}{n_o} = \frac{e}{T_e}\exp(im\theta-in\zeta-i\omega t)\sum_{p,p'} a_{p'}N_{pp'}\exp(ip\theta),$$

where

$$N_{pp'} = \delta_{pp'} - \frac{1}{2\pi}\int_0^{2\pi} d\theta e^{-ip\theta}\int_T d^3\underset{\sim}{v}\,\frac{(\omega-\omega_{*e})F_e^M\langle\exp(ip'\theta)\rangle}{\omega-\omega_d(\lambda,v)+i\nu_{eff}(v)}, \tag{14}$$

c. Dispersion Relation

Applying the quasi-neutrality condition we obtain the matrix equation

$$\sum_{p'} \left[\tau M_{pp'}(\omega) + N_{pp'}(\omega) \right] a_{p'} = 0. \qquad (15)$$

The dispersion relation is

$$\det \left[\tau M_{pp'}(\omega) + N_{pp'}(\omega) \right] = 0. \qquad (16)$$

Once ω is obtained from (16) the poloidal mode structure can be found from (15). Of course, in practice, one must do this by truncating the infinite matrix to a finite matrix. This program has been carried out for a specific model equilibrium (described in Sec. IV) and the results are reported in Sec. V.

IV. EQUILIBRIUM

To evaluate the various quantities involved in the dispersion relation and, in particular, the toroidal drift frequency ω_d, we first establish a solution to the magnetohydrodynamic equilibrium equation:

$$\left(\frac{\partial^2}{\partial R^2} - \frac{1}{R}\frac{\partial}{\partial R} + \frac{\partial^2}{\partial z^2}\right)\psi = -4\pi R^2 \frac{\partial}{\partial \psi} p - \frac{1}{2}\frac{\partial}{\partial \psi}(RB_\zeta)^2, \qquad (17)$$

where z is the vertical coordinate normal to the toroidal plane and p is the plasma pressure. Following Reference 2, we specialize to a particular analytical model equilibrium, namely, an equilibrium in whch the magnetic surfaces are nested ellipses of the same ellipticity, κ, and the toroidal current density is constant (i.e., the right hand side of Eq. (17) is constant. Letting $x \equiv R-R_o \ll R_o$, Eq. (17) reduces to

$$\left(\frac{\partial^2}{\partial x^2} + \frac{\partial^2}{\partial z^2}\right)\psi = \text{constant}. \qquad (18)$$

Equation (18) yields the solution

$$\psi = \kappa B_o \rho^2/2q, \qquad (19)$$

where $x = \rho\cos\theta$ and $z = \kappa\rho\sin\theta$, B_o is the magnetic field at $\rho = 0$ and q is constant. It is easy to show that the coordinate θ

defined in Sec. III is the same as the elliptical parameter θ defined above.

The bounce period τ_b and the longitudinal adiabatic invariant J can now be written:

$$\tau_b = q(B_o v)^{-1} \oint d\theta \; RB(1-\lambda B)^{-\frac{1}{2}}, \tag{20}$$

$$J = qvB_o^{-1} \oint d\theta \; RB(1-\lambda B)^{\frac{1}{2}}, \tag{21}$$

where $R = R_o + \rho \cos\theta$, $B \approx B_o \left\{ 1 - \varepsilon \cos\theta + \varepsilon^2 \cos^2\theta + \frac{1}{2} \varepsilon^2 q^{-2} \left[1 + (\kappa^2 - 1) \cos^2\theta \right] \right\}$, and $\varepsilon \equiv \rho/R_o$.

The reflection positions (i.e., the points where $v_\parallel = 0$), θ_c, for a trapped particle with pitch angle variable λ is determined by the equation

$$\lambda B(\theta_c) = 1. \tag{22}$$

If κ is sufficiently large such that $2\varepsilon + (\kappa^2-1)\,\varepsilon q^{-2} > 1$, the trapped particles will assume two types of orbit:

(i) If $\lambda B(\theta = 0) < 1$, Eq. (22) allows only one positive solution for θ_c ($<\pi$), hence the trapped particles bounce between $-\theta_c$ and θ_c, as in the case of circular cross section tokamaks.

(ii) If $\lambda B(\theta = 0)>1$, Eq. (19) allows two positive solutions, $\theta_c^{(1)}$ and $\theta_c^{(2)}$, and the trapped particles will bounce between $\theta_c^{(1)}$ and $\theta_c^{(2)}$, or between $-\theta_c^{(1)}$ and $-\theta_c^{(2)}$.

Substituting Eqs. (19)-(22) into Eq.(13) and expanding in terms of ε, we obtain

$$\omega_d = \frac{nm_e cv^2}{eB_o\rho^2} h(\lambda,q,\varepsilon)$$

where

$$h(\lambda,q,\varepsilon) \equiv - \frac{\int d\theta\, \chi_1/\chi_2}{\int d\theta \chi_3}$$

$$\chi_1 \equiv \frac{1}{2} \lambda B_o q\kappa^{-1}\left\{-\varepsilon q^{-1}\cos\theta + 2\varepsilon^2\cos^2\theta + \varepsilon^2 q^{-2}\left[1+(\kappa^2-1)\cos^2\theta\right]\right\}$$

$$- \varepsilon^2\kappa^{-1}q^{-1}(1-\lambda B)\left[1 + (\kappa^2-1)\cos^2\theta\right]\left\{1+\frac{1}{2}\varepsilon^2 q^{-2}\left[1+(\kappa^2-1)\cos^2\theta\right]\right\},$$

$$\chi_2 \equiv (1-\lambda B)^{\frac{1}{2}}\left\{1-\frac{1}{2}\varepsilon^2 q^{-2}\left[1+(\kappa^2-1)\cos^2\theta\right]\right\},$$

$$\chi_3 \equiv \left\{1 + \frac{1}{2}\varepsilon^2 q^{-2}\left[1 + (\kappa^2-1)\cos^2\theta\right]\right\}(1-\lambda B)^{-\frac{1}{2}}.$$

Figure 1 shows h as a function of λB_{min} for $q = 2$, $\varepsilon = 0.25$, and several values of κ, where B_{min} is the minimum magnetic field on the flux surface $\varepsilon = 0.25$. Note that for $\kappa \geq 3.5$, all trapped electrons have negative toroidal drift.

V. RESULTS

As shown in Eq. (16), the full dispersion relation is the determinant of an infinite matrix, each element of which is an infinite sum resulting from the ion orbits. This together with the fact that the growth rate γ is generally comparable to the frequency ω_r renders the usual perturbation techniques useless for obtaining an approximate analytical solution of Eq. (16). We have therefore numerically evaluated Eq. (16) for the model equilibrium of Sec. IV. The infinite sum in $M_{pp'}$ [Eq. (12)] is evaluated by including as many terms as needed. Excellent convergence is always obtained by truncating the sum at $|s| \leq 10$. Finally the determinant is truncated at the point of convergence (typically a 7x7 matrix is sufficient) and evaluated. Two checks have been made to insure that the mode with maximum growth rate has not been left out. First, the Nyquist technique was used to monitor the number of roots. Secondly, in the limit of low mode number $\left[\alpha \ll 1, \text{ see Eq. (9)}\right]$, the matrix in Eq. (16) is essentially diagonal and the root reduces to the root of the first diagonal element as expected. Since $\gamma \ll \omega_r$ in this limit, the numerical value of the root can also be checked against approximate analytical expressions.

In what follows, we assume a hydrogen plasma with $T_e = T_i$, $\eta_e = \eta_i = 1$, $\epsilon \equiv \rho/R_o = 0.25$, $q = 2$, and $Z_{eff} = 2$. The density scale length $L_n \equiv -n_o(dn_o/d\rho)^{-1}$ is specified as $L_n = 0.2R_o$. The parameters B_o, n_o, and T_e can be scaled out of Eq. (16), if

we normalize ω, ω_*, and ν_{eff} with respect to the electron bounce frequency (ω_{be}) and treat ν_* ($\equiv \nu_{eff}/\omega_{be}$) and $nq\rho_i/\rho$ as variable parameters, where $\rho_i = v_i m_i c/eB_o$ and n is the toroidal mode number. However, to be specific, we let B_o = 45 kG, $n_e = 5x10^{13}$ cm^{-3} and treat T_e and n as variable parameters instead. (The data so obtained can be converted into the more general representation as described above.) With these parameters specified, we now solve Eq. (16) for ω ($= \omega_r + i\gamma$), varying the parameters κ, T_e, and n. Figure 2 shows plots of the growth rate maximized over mode number versus electron temperature for several different values of κ. Figures 3a and b, which display ω_r and γ as a function of n for $T_e = T_i$ = 3 keV, are typical dispersion curves. From Fig. 2, we note that for κ = 2, 3, and 4, the maximum growth rates are reduced by factors of 0.8, 0.6, and 0.4, respectively, as compared to the circular case (κ = 1), and this is approximately independent of electron temperature. Although these growth reductions are modest, they may still be significant since they imply that the amount of shear necessary to stabilize the mode is correspondingly reduced.[6] Furthermore, Fig. 3b shows that the mode number for which γ peaks increases as the ellipticity increases. This might be significant if, as is sometimes argued (e.g. turbulent diffusion $\sim \gamma/k^2$), the short wavelength modes are less dangerous than the long wavelength modes. We note that although the electron toroidal drift has been reversed for all electrons

for $\kappa = 4$, there is still no dramatic stabilization of the mode. This might be because for $\kappa = 4$ there exist modes with reversed toridal phase velocity (cf. Fig. 3 which shows a region of negative ω_r for $n \geq 290$.)

It is interesting to note that some equilibrium studies[7] show that even if the elongation of the plasma boundary is modest, the interior magnetic surfaces can become very elongated.

One of us (KRC) would like to thank Dr. A. T. Drobot, Dr. I Haber, Dr. W. E. Hobbs, and Dr. W. Jones for helpful discussions on the numerical aspect of the problem. This work was supported by the U.S. Energy Research and Development Administration.

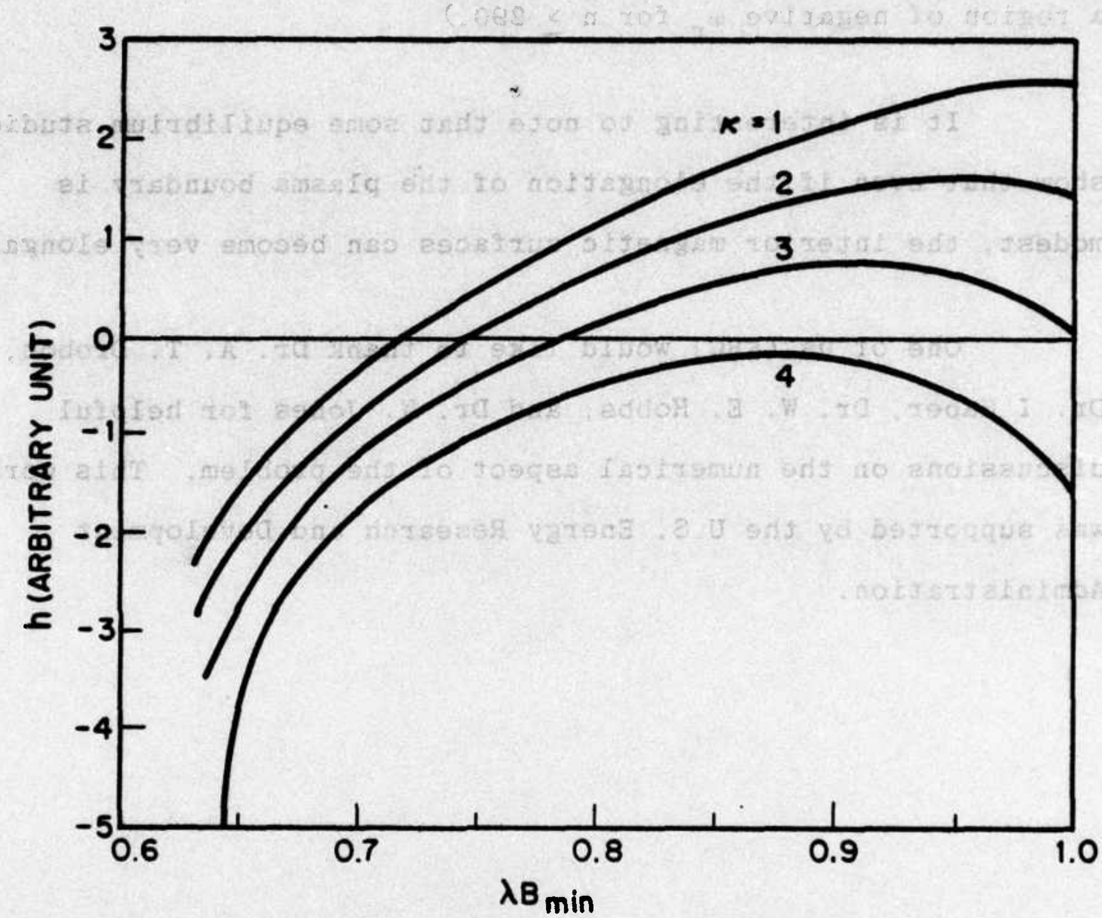

Fig. 1 — $h(\lambda, q, \epsilon)$ versus λB_{min} for trapped particles. $\epsilon = 0.25$, $q = 2$.

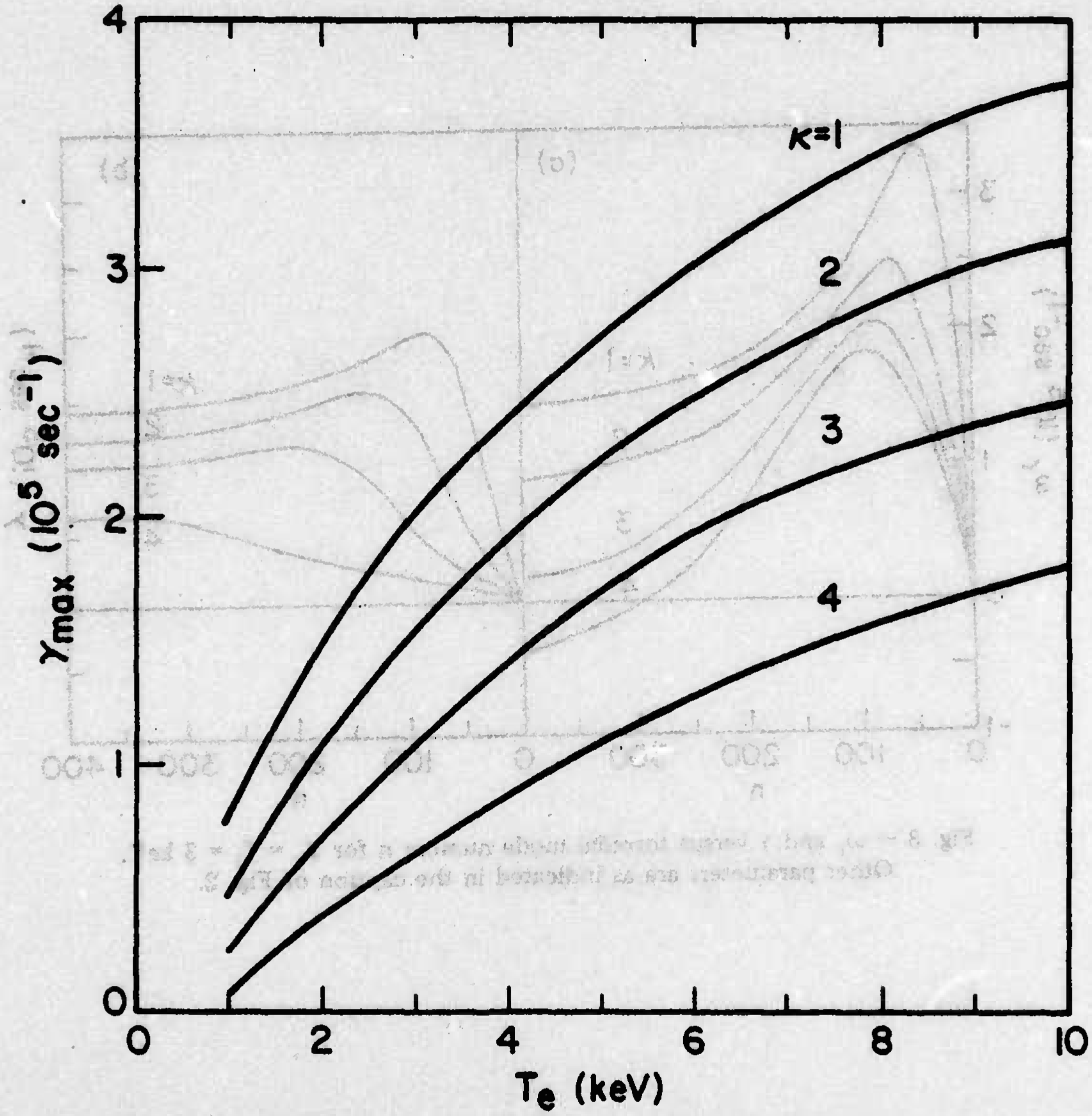

Fig. 2 — γ_{max} (growth rate maximized over mode number) versus T_e for different values of κ. Parameters for this figure are: $B_o = 45$ kG, $\epsilon = 0.25$, $L_n/R_o = 0.2$, $q = 2$, $n_o = 5 \times 10^{13} cm^{-3}$, $Z_{eff} = 2$, and $\eta_e = \eta_i = 1$.

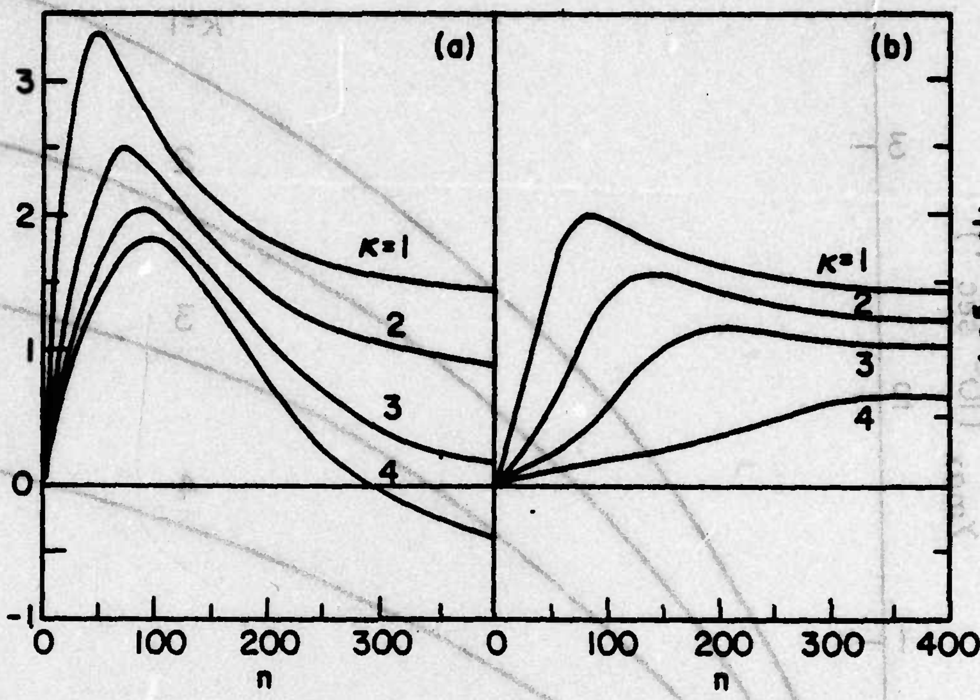

Fig. 3 — ω_r and γ versus toroidal mode number n for $T_e = T_i = 3$ keV. Other parameters are as indicated in the caption of Fig. 2.

REFERENCES

1. J. C. Adam, W. M. Tang and P. H. Rutherford, Phys. Fluids 19, 561 (1976), also W. M. Tang, P. H. Rutherford, H. P. Furth, and J. C. Adam, Phys. Rev. Lett. 35, 660 (1975).
2. A. H. Glasser, E. A. Freiman and S. Yoshikawa, Phys. Fluids 17, 181 (1974).
3. E. Ott, W. M. Manheimer, and K. R. Chu (to be published).
4. B. B. Kadomtsev and O. P. Pogutse, Doklady Akad. Nauk SSSR 186. 553 (1969) [Soviet Phys. - Doklady 14, 470 (1969)].
5. L. Spitzer, Jr., Physics of Fully Ionized Gases (Interscience, New York, 1962) p. 132.
6. It is shown in Ref. 3 that shear induced damping rate is almost independent of ellipticity.
7. J. P. Friedberg, Bull. Am. Phys. Soc. 21, 1033 (1976).

TOROIDAL CTR DISTRIBUTION LIST
UNCLASSIFIED

1. Oak Ridge National Laboratory
   P. O. Box X
   Oak Ridge, Tennessee 37830

   Attn: J. Clarke
   J. Callen
   J. Hogan
   D. McAlees
   M. Roberts
   J. Rome
   G. Bateman
   C. Beasley
   R. Dory
   C. Crume

2. E. R. D. A.
   Germantown, Maryland 20767

   Attn: S. O. Dean (3 copies)
   G. Hess
   R. L. Hirsch (3 copies)
   B. Miller (3 copies)
   R. Blanken
   R. Price (3 copies)
   W. Sadowski
   D. Priester
   A. Sleeper
   A. Davies

3. Lawrence Livermore Laboratory
   University of California
   Livermore, California 94551

   Attn: T. K. Fowler
   D. Baldwin
   H. Berk
   J. Killeen
   B. McNamara
   R. Post
   J. Byers
   W. Kruer
   E. Valeo
   B. Langdon

4. Massachusetts Institute of Technology
   77 Massachusetts Avenue
   Cambridge, Mass. 02139

   ATTN: B. Coppi (Physics)
   T. H. Dupree (Nuc. Eng)
   A. Bers (E. E.)
   D. Sigmar (Nuc. Eng.)
   J. McCune (A. E.)
   R. Parker (E. E.)

5. U. C. L. A.
   Los Angeles, California 90024

   Attn: J. Dawson
   B. Fried
   Y. C. Lee
   F. F. Chen (E. E.)

6. Princeton University
Plasma Physics Laboratory
Princeton, New Jersey 08540

Attn: M. B. Gottlieb
R. Ellis
E. Frieman
H. Furth
D. Grove
D. Meade
R. Mills
P. Rutherford
T. Stix
D. Jassby
W. Tang
F. Perkins
J. Johnson
R. Kulsrud
H. Okuda
T. K. Chu
C. Oberman
J. M. Greene

7. Los Alamos Scientific Laboratory
P. O. Box 1663
Los Alamos, New Mexico 87344

Attn: F. L. Ribe
D. Forslund
C. Nielson
J. Friedberg
R. Morse
J. Kindell
B. Godfrey
R. Mason
W. Ellis
E. Lindman
H. R. Lewis
J. U. Brackbill

8. University of Texas
Austin, Texas 78712

Attn: D. Ross
W. Drummond
A. Ware
L. Sloan
F. Hinton
W. Horton
R. Hazeltine

9. University of California
Berkeley, California 94720

Attn: Prof. A. Kaufman
Prof. C. K. Birdsall

10. Bell Telephone Laboratories
Shippany, New Jersey 07981

Attn: S. Buchsbaum
A. Hasegawa

11. National Science Foundation
Washington, D. C. 20550

Attn: E. C. Creutz
R. Sinclair

12. General Atomic Co.
P. O. Box 81608
San Diego, California 92138

Attn: T. Ohkawa M. S. Chu
D. Dobrott
G. Guest

13. Westinghouse Electric Company
Breeder Reactor Division
P. O. Box 355
Pittsburgh, Pennsylvania 15230

Attn: Z. Shapiro
D. Klein
R. Rose
T. Varljen

14. University of Wisconsin
Madison, Wisconsin 53706

Attn: R. Conn
G. Kulcinski

15. New York University
Courant Institute of Math. Sci.
251 Mercer St.
New York, N. Y. 10012

Attn: H. Grad
W. Grossman
H. Weitzner
J. Tataronis

16. Maxwell Laboratories, Inc.
9244 Balboa Ave.
San Diego, CA 92123

Attn: A. Kolb
V. Fargo
N. Rostoker

17. Institute for Advanced Study
Olden Lane
Princeton, New Jersey 08540

Attn: M. Rosenbluth

18. Batelle
Pacific Northwest Lab.
P. O. Box 999
Richland, Washington 99352

Attn: L. Schmidt

19. Forsen Incorporated
777-106 Avenue, N. W.
Bellevue, Washington 98004

Attn: H. Forsen

20. University of Maryland
College Park, Maryland 20742

Attn: P. C. Liewer
Prof. R. Davidson
C. S. Liu
H. Griem
D. Tidman

21. Stevens Institute of Technology
Hoboken, New Jersey 07030

Attn: George Schmidt
B. Rosen

22. College of William and Mary
Williamsburg, Virginia 23185

Attn: S. P. Gary
Fred Crownfield

23. Culham Laboratory
Abingdon, Berkshire, England

Attn: Chris Lashmore Davies
Ian Cook
Keith Roberts
Jes Christiansen
J. B. Taylor
B. Peas
M. Hughes
J. A. Wesson
T. Stringer
J. W. M. Paul
A. Gibson

24. Sandia Laboratory
Albuquerque, New Mexico 87115

Attn: Thomas Wright
J. Freeman

25. University of Rochester
Rochester, New York 14627

Attn: Moishe Lubin
E. B. Goldman
P. J. Catto

26. Max Planck Institute fur Plasma Physics
8046 Garching bei Munchen
West Germany

Attn: D. Biskamp
Horst Pacher
W. Schneider
K. Von Hagenow
Chodura
D. Pfirsch

27. Physics International Company
San Leandro, California 94577

Attn: V. Bailey

28. Science Applications, Inc.
Laboratory for Applied Plasma Physics
Research Staff
La Jolla, California 92037

Attn: N. Krall
R. Shanny
J. McBride
C. Wagner
H. Klein
N. Byrne

29. University of Tokyo
Bunkyo-ku
Tokyo, Japan 113

Attn: Soichi Yoshikawa

30. Japan Atomic Energy Research Institute
Tokai-Mura
Ibaraki-Ken, Japan

Attn: N. Fujisawa

31. Association Euratom-CEA Serv La Fusion
Dept. of Physics du Plasma et de la
Fusion Controlee
Center d'Etudes Nucleaires
Boite Postale No 6
92260 Fontenay-Aux-Rose
France

Attn: Dr. Tachon
Dr. Mercier
R. B. Paris

32. Australian National University
Canberra A. C. T. Australia

Attn: J. D. Strachan
R. L. Dewar

33. Kurchatov Institute
Moscow, U. S. S. R.

Attn: B. B. Kadomtsev
E. P. Velikov

34. Cornell University
Ithaca, New York 14850

Attn: Prof. R. N. Sudan (App. Phys.)
Prof. E. Ott (E. E.)
R. V. Lovelace

35. Naval Research Laboratory
Washington, D. C. 20375

Attn: Code 7700 (Tena Mason) - 25 copies
Code 7750 - 75 copies

DEPARTMENT OF THE NAVY

NAVAL RESEARCH LABORATORY
Washington, D.C. 20375

OFFICIAL BUSINESS
PENALTY FOR PRIVATE USE, $300

POSTAGE AND FEES PAID
DEPARTMENT OF THE NAVY
DoD-316

LME